The Cercarial Glycocalyx of *Schistosoma mansoni*

JOHN C. SAMUELSON and JOHN P. CAULFIELD
Department of Pathology and Division of Tropical Medicine, Brigham and Women's Hospital and the Harvard Medical School, Boston, Massachusetts 02115

ABSTRACT Cercariae, the freshwater stage of *Schistosoma mansoni* infectious to man, are covered by a single unit membrane and an immunogenic glycocalyx. When cercariae penetrate the host skin, they transform to schistosomula by shedding tails, secreting mucous and enzymes, and forming microvilli over their surface. Here the loss of the glycocalyx from cercariae transforming in vitro was studied morphologically and biochemically. By scanning electron microscopy, the glycocalyx was a dense mesh composed of 15–30 nm fibrils that obscured spines on the cercarial surface. The glycocalyx was absent on organisms fixed without osmium and was partially lost when parasites aggregated in their own secretions before fixation. By transmission electron microscopy, a 1–2-μm thick mesh of 8–15-nm fibrils was seen on parasites incubated with anti-schistosomal antibodies or fixed in aldehydes containing tannic acid or ruthenium red. Cercariae transformed to schistosomula when tails were removed mechanically and parasites were incubated in saline. Within 5 min of transformation, organisms synchronously formed microvilli which elongated to 3–5 μm by 20 min and then were shed. However, considerable fibrillar material remained adherent to the double unit membrane surface of schistosomula. For biochemical labeling, parasites were treated with eserine sulfate, which blocked cercarial swimming, secretion, infectivity, and transformation to schistosomula. Material labeled by periodate oxidation and NaB^3H_4 was on the surface as shown by autoradiography and had an apparent molecular weight of $>10^6$ by chromatography. Periodate-NaB^3H_4 glycocalyx had an isoelectric point of 5.0 ± 0.4 and was precipitable with anti-schistosomal antibodies. More than 60% of the radiolabeled glycocalyx was released into the medium by transforming parasites in 3 h and was recovered as high molecular weight material. Parasites labeled with periodate and fluorescein-thiosemicarbazide and then transformed had a corona of fluorescence containing microvilli, much of which was shed onto the slide. Material on cercariae labeled by Iodogen-catalyzed iodination was also of high molecular weight and was antigenic. In conclusion, the cercarial glycocalyx appears to be composed of acidic high molecular weight fibrils which are antigenic and incompletely cleared during transformation.

The helminth parasite *Schistosoma mansoni* undergoes a series of adaptive changes as it moves from its intermediate snail host to man. Cercariae are shed from the snail into fresh water, where they swim until they find a host. Cercariae are composed of a body (CB) and a tail, each ~120 μm long and 25 μm in diameter. The CB contains excretory, nervous, and digestive systems, and large secretory glands, all of which are surrounded by two muscle layers (54). The outermost layer of the parasite is a syncytium called the tegument, which is connected to cell bodies beneath the musculature (20). The cercarial tegument is bounded by a single unit membrane with a surface area of 20,000 μm^2 over the CB (43), and a thick, periodic acid Schiff-positive glycocalyx (24, 53).

Cercariae that penetrate a host undergo a set of changes called transformation (54). The tail is lost and the secretory glands release both a mucus, which promotes attachment to the skin, and enzymes, which degrade the skin (17, 54). In addition, transient microvilli appear on the surface and a double unit membrane is formed on the tegument (20). At the same time, some of the glycocalyx is lost (20, 53). Transformation is complete in ~3 h. The parasites are called schistosomula. Transformation can also be produced in vitro when parasites penetrate excised skin (56) or when tails are removed mechanically and CBs are incubated in physiological media (6, 38).

The surface of cercariae and schistosomula is immunolog-

ically important. The cercarial glycocalyx binds antibodies from humans and laboratory animals infected with *S. mansoni* (25, 26, 51, 55, 59). The surfaces of both cercariae (8) and newly transformed schistosomula (11, 39) activate complement by the alternative pathway. In vitro, schistosomula are killed by human eosinophils and rodent granulocytes in antibody-dependent reactions during the first 24–48 h after transformation (3, 10, 36). Later, the schistosomula become resistant to antibody-mediated killing (10, 32, 39). The composition and amount of antigenic glycocalyx retained after transformation are, therefore, of major interest.

The lack of biochemical data on the cercarial glycocalyx is due to difficulties in handling the parasite. Cercariae swim at a rate of 2 mm/s and so resist centrifugation. Furthermore, the parasites secrete mucus and aggregate, so they cannot be easily separated (24, 38, 55). Therefore, in the labeling studies performed here, cercarial swimming and secretion were inhibited with eserine sulfate (ES[1]; reference 1). In addition, ES reversibly inhibits transformation.

The cercarial glycocalyx was studied morphologically and biochemically. First, we examined the glycocalyx by scanning microscopy to allow comparison with previous transmission microscopy observations and to follow the structure through transformation. Second, we labeled immobilized cercariae with sodium metaperiodate (Per) and NaB^3H_4 (15, 43) and determined the distribution of the label by light microscopic autoradiography (LMARG). The molecular weight and isoelectric point of the radiolabeled material were also determined, as was as its loss during transformation. Third, we examined transformation by fluorescence microscopy by labeling the glycocalyx first with periodate then with fluorescein-thiosemicarbazide (FITSC; reference 16). Alternatively, the glycocalyx was labeled with fluorescent anti-schistosomal antibodies (4), or the new schistosomular membrane was labeled with fluorescent concanavalin A (FIConA; reference 45).

MATERIALS AND METHODS

Reagents: Artificial pond water (APW) contained 50 mg $CaCl_2$, 120 mg $MgSO_4$, 15 mg $FeCl_3$, and 4 mg K_2SO_4 in 1 liter distilled water, buffered with 20 mM HEPES, pH 7 (23). Phosphate-buffered saline (PBS) contained 0.01 M sodium phosphate, pH 7.2, and 0.14 M NaCl. Hank's balanced salt solution, Earles' minimal essential medium, RPMI-1640, and Earles' lactalbumin were purchased from M.A. Bioproducts (Walkersville, MD), and buffered with 10 mM HEPES, pH 7.2. Per, ES, serotonin, RNAse, DNAse, and EDTA were purchased from Sigma Chemical Co. (St. Louis, MO); Iodogen from Pierce Chemical Co. (Rockford, IL); NaB^3H_4 (6–10 Ci/mM) and $Na^{125}I$ (15 Ci/mg) from Amersham Corp. (Arlington Heights, IL); FITSC from Molecular Probes (Junction City, OR); FICon A from Vector Laboratories, Inc. (Burlingame, CA); tannic acid from Mallinckrodt Inc. (Paris, KY); ruthenium red from Electron Microscopy Sciences (Fort Washington, PA); NTB2 emulsion and Tri-X 35-mm film from Eastman Kodak (Rochester, NY); SDS and Nonidet P40 (NP40) from BDH Chemicals (Poole, England); guanidine hydrochloride and urea from Schwartz/Mann (Spring Valley, NY): Zwittergent detergent from CalBiochem-Behring Corp. (LaJolla, CA); Percoll, Sepharose CL-2B, protein A-Sepharose, Ampholytes (pH 3–10), and molecular weight standards from Pharmacia Fine Chemicals (Piscataway, NJ); polyacrylamide and Bio-Lyte gels from Bio-Rad Laboratories (Richmond, CA); and Bio-Fluor from New England Nuclear (Boston, MA).

Preparation of Parasites: A Puerto Rican strain of *S. mansoni* was carried in *Biomphalaria glabrata* snails and CBA/J mice (Jackson Laboratory, Bar Harbor, ME). Cercariae in APW were shed from infected snails for 1–2 h at room temperature. We prepared CBs mechanically in 0.01 M sodium phosphate by either shearing through a 23 gauge needle at room temperature (5), or by chilling them on ice and vortexing (38).

Transformation to Schistosomula: 2,000–10,000 cercariae and CBs/ml were transformed to schistosomula by incubation in APW, PBS, Hank's balanced salt solution, Earles' minimum essential medium, or RPMI-1640, all at 37°C. Parasites were judged to be transformed if microvilli covered their surface after 10 min incubation when viewed at 10,000X with the scanning microscope. We determined the density of microvilli on transforming organisms by counting villi within 6-μm^2 areas of the parasite surface at 30,000X; the lengths of microvilli were measured at 40,000X. Skin schistosomula were harvested 3 h after penetration through an excised rat skin into Earles' lactalbumin (56). The viability of parasites was monitored by observations of wiggling, flame cell beating, and lack of blebbing, and was >95% for all preparations.

^3H, Fluorescein, and ^{125}I Labeling: Cercariae or CB were immobilized with 1 mM ES (1) and purified on a 50 ml of 0.01 M sodium phosphate and 25 or 40% Percoll, respectively (29). 1,000–10,000 organisms/ml 0.01 M sodium phosphate were incubated with 5 mM Per for 10 min at 4°C, washed, and then incubated with 0.5–1.0 mCi NaB^3H_4 for 30 min at room temperature (15, 43). Alternatively, Per-treated organisms were incubated with 100 μg/ml FITSC for 30 min at room temperature (16). As a control, untreated organisms were incubated with NaB^3H_4 or FITSC. Parasites were also incubated for 10 min at 4°C with 0.5–1.0 mCi $Na^{125}I$ in scintillation vials previously coated with 150 μg Iodogen (31). Radiolabeled parasites were washed eight times and immediately solubilized for chromatography. Alternatively, 2,000–10,000 CBs were transformed to schistosomula in 300 μl RPMI for 1–3 h, and organisms were separated from the medium by centrifugation. For chromatography, SDS or urea was added directly to the medium.

Autoradiography: LMARG and grain counts to localize radioactivity on Per-NaB^3H_4– and $Na^{125}I$–treated parasites were performed by use of NTB2 emulsion as previously described (43).

SDS PAGE: Parasites were boiled for 2 min in 1% SDS, 2% β-mercaptoethanol, and 0.01 M Tris, pH 6.8, and were electrophoresed in 13-cm tubes containing 5% acrylamide in the running gels and 3% acrylamide in the stack (28). Other samples were solubilized and electrophoresed in phosphate-buffered SDS (60). Gels were sliced and counted in Bio-Fluor as previously described (43). We estimated the efficiency of counting by measuring external standard ratios and comparing with quenched tritium standards.

Column Chromatography: Per-NaB^3H_4–labeled parasites were solubilized in 150 μl of buffer containing 4 M guanidine, 1% Zwittergent, and 0.1 M Tris, pH 7.0. Samples were chromatographed on a 100 × 0.6 cm column of Sepharose CL-2B at a flow rate of 2 ml/min (14). Per-FITSC–labeled organisms were also chromatographed and fractions were measured for fluorescein with a fluorimeter.

Immune Precipitations: The IgG fraction of serum from a rabbit hyperimmunized to *S. mansoni* (IRS) by repeated injections of schistosome homogenate in Freund's adjuvant was purified and provided by Dr. Donald Harn, Harvard Medical School. Per-NaB^3H_4– and Iodogen-$Na^{125}I$–labeled parasites were solubilized in PBS containing 0.1% NP40 and incubated for 60 min at room temperature with protein A-Sepharose, which was precoated with IRS or with normal rabbit IgG (NRS) as a control (27). We washed the Sepharose and eluted the precipitated radioactivity by boiling it in 1% SDS.

Isoelectric Focusing: 2,000–10,000 Per-NaB^3H_4 labeled organisms were incubated in 1% NP40, 50 μg/ml RNAse, and 1 mg/ml DNAse for 10 min at 4°C, spun to remove insoluble material, and 8 M urea, 2% β-mercaptoethanol, and 2% Ampholytes were added (35). 20-μl samples were focused on an 11-cm flatbed isoelectric focusing gel containing 8 M urea, 1% NP40, 4% Ampholytes, and 4% Bio-Lyte for 40,000–80,000 V·h (37). 1-cm^2 samples were cut out, incubated with 1 ml distilled water, and then counted in a scintillation counter or measured with a pH meter. Alternatively, samples were focused on a 100-ml column containing urea, Ampholytes, NP40, and a gradient of sucrose from 0–20%.

Fluorescence Microscopy and Photometry: Parasites were labeled with Per-FITSC, rhodamine-conjugated IRS (4), or FICon A (45). Fluorescent parasites were observed with a Leitz Orthoplan microscope equipped with a Ploem illumination system for fluorescein or rhodamine, and Smith-T interference-contrast optics (E. Leitz, Inc., Rockleigh, NJ). Parasites were photographed with Tri-X film at 1600 ASA. The fluorescence of a 200-μm^2 area of ES-treated parasites labeled with FITSC was measured with a Leitz MPV Compact photometer attached to the fluorescence microscope (45).

Scanning Microscopy: Parasites were fixed for 20 min on ice with 2% glutaraldehyde and 2% osmium tetroxide in 0.1 M sodium phosphate, pH

[1] *Abbreviations used in this paper*: APW, artificial pond water; CB, cercarial body; ES, eserine sulfate; FICon A, fluorescein-conjugated concanavalin A; FITSC, fluorescein-thiosemicarbazide; IRS, IgG fraction of serum from a rabbit hyperimmunized to *S. mansoni*; LMARG, light microscopic autoradiography; NP40, Nonidet P40; NRS, normal rabbit IgG; Per, sodium metaperiodate.

7 (19). Alternatively, organisms were fixed for 30 min on ice with 1% formaldehyde and 3% glutaraldehyde in 0.1 M cacodylate, pH 7.4 (22), with or without postfixation in 1% osmium on ice for 60 min. Parasites were then dehydrated in graded alcohols, critical-point dried, and sputter-coated (44).

Transmission Microscopy: Parasites were fixed in mixed aldehydes for 30 min on ice (22), postfixed in osmium for 90 min on ice, stained en bloc with uranyl acetate for 2 h at room temperature, dehydrated, and embedded (50). Some parasites were preincubated with 1 mg/ml IRS or NRS for 1 h at room temperature, and washed four times before fixation in mixed aldehydes (4). Alternatively, parasites were fixed in glutaraldehyde containing ruthenium red (30) or tannic acid with or without 0.5 mg/ml saponin (34), and postfixed with osmium. Thin sections were cut with a diamond knife and stained on grid with 4% uranyl acetate for 5 min at room temperature and lead citrate for 1 min (41). Scanning and transmission samples were examined with a JEOL 100C-ASID electron microscope.

Repetition of Experiments: Each experiment was repeated at least three times.

RESULTS

Cercarial Transformation

More than 90% of cercariae synchronously transformed to schistosomula when tails were removed and organisms were placed into PBS, Hank's balanced salt solution, Earles' minimum essential medium, or RPMI, whereas only 10 ± 6% of tailed organisms transformed. CBs were inhibited from transforming by APW, 1 mM ES, or 10 mM EDTA. However, 80 ± 5% of CBs transformed when ES was removed. In 1 mM serotonin, 59 ± 16% of CBs transformed. Therefore, in the studies below, CBs were used to observe the ultrastructure of transformation and parasites were immobilized with ES for biochemical labeling.

Microscopy of the Cercarial Surface

The surfaces of whole cercariae and of tailless CB look the same, so they are described together. The surface of cercariae in APW also looked the same when fixed with glutaraldehyde and osmium or with mixed aldehydes and then postfixed with osmium. The glycocalyx appeared as a meshwork of 15–30-nm fibrils that covers the spines (Figs. 1–3) except on the anterior tip of the parasites. When osmium was omitted during fixation, the meshwork was absent, and naked spines and pits 0.2–0.4 μm in diameter were seen on the parasite body (Fig. 4). Parasites that were aggregated by their glandular secretions (Fig. 5) had less glycocalyx than either unaggregated parasites or organisms in which secretion was blocked with ES. Cercarial tails had a fibrillar mesh identical to that seen on the body, but the tips of spines were often visible. However, in the absence of osmium, no pits were seen on the tail.

As shown by transmission microscopy, the cercarial glycocalyx is a 1–2-μm-thick fibrillar mesh covering the entire tegument of organisms preincubated in IRS and fixed with aldehydes and osmium (Figs. 6 and 7). Organisms fixed without preincubation in IRS, or after preincubation in NRS, did not have a visible glycocalyx (Fig. 8). The glycocalyx also appeared as a mesh of 8–15-nm fibrils on parasites fixed in aldehydes containing either tannic acid (Fig. 9) or ruthenium red (Fig. 10). The cercarial tegument was covered by a single unit membrane beneath the glycocalyx (Figs. 9 and 10).

Scanning and Transmission Microscopy of Cercarial Transformation to Schistosomula

Microvilli covered the entire surface of transforming CBs (Fig. 11). 5 min after the start of transformation (Fig. 12), microvilli barely projected through the dense glycocalyx. After 10 min (Fig. 13) and 20 min (Fig. 14), the microvilli were 1–2 μm and 3–5 μm long, respectively. There were 2.0 ± 1.2 microvilli/μm^2 surface area, and the density remained constant over time. Fibrils of glycocalyx extended between microvilli, some of which were covered by 15–30-nm spheres (Figs. 13 and 14). After 40–60 min, microvilli were lost from much of the surface of transforming CBs (Fig. 15). However, the glycocalyx still covered spines on the middle and posterior of CBs. 3 h after transformation, spines projected through fibrillar material on the surface of mechanically and skin-prepared schistosomula (Fig. 16). Tails in RPMI did not form microvilli and did not shed their glycocalyx. Transforming parasites fixed without osmium had no glycocalyx on spines and microvilli (Fig. 17).

By transmission microscopy, microvilli were 100–150 nm in diameter, were bound by a single unit membrane, and had a thick coat of glycocalyx (Figs. 18–20). Simultaneous with microvilli formation, multilaminate vesicles entered the tegumental cytoplasm from cell bodies beneath the muscle and discharged onto the parasite surface (Figs. 18 and 19). The tegument was covered in part by a pentalaminar, double unit membrane at 10–30 min (Fig. 21). A double membrane covered the entire surface at 60–120 min (Fig. 22). Residual glycocalyx overlay the double membrane and varied in thickness from <0.1–0.5 μm (Fig. 22).

Labeling with Periodate and Tritiated Borohydride

Per-NaB^3H_4–treated cercariae incorporated 25 times the radioactivity of unoxidized controls. The amount of radioactivity on cercariae, 52 ± 15 dpm/organism (mean ± SD), was equivalent to ~3×10^9 NaB^3H_4-reduced molecules/organism or 1.5×10^5 molecules/μm^2 area of the parasite surface. LMARG showed that on Per-NaB^3H_4–labeled cercariae the surface grain density was 34 times that of the interior (Table I). Surface grains accounted for 92% of the total grains on Per-NaB^3H_4 cercariae. In contrast, on unoxidized organisms, surface grain density approximated that of the interior and accounted for only 21% of the total radioactivity. By scanning and transmission microscopy, there was no alteration in the glycocalyx or the surface membrane after Per-NaB^3H_4 labeling.

On reduced SDS PAGE, most Per-NaB^3H_4–labeled material on cercariae and CBs was retained in the stack (Fig. 23). This high molecular material was not labeled on organisms treated with NaB^3H_4 alone and was precipitated by IRS but not by NRS (Fig. 24). On Sepharose 2B, 70–90% of the radioactivity on cercariae eluted in the void volume (V_0) with a broad shoulder extending to R_f 0.5, whereas the remaining label eluted with the total volume (V_t; Fig. 25). Label on isolated tails eluted with an R_f of 0.2–0.3, which was slightly behind material from CB. On the same column, dextran of 2×10^6 mol wt had a peak with an R_f of 0.5–0.6. Radioactivity on unoxidized organisms eluted entirely in V_t. Per-NaB^3H_4 material had an isoelectric point of 5.0 ± 0.4 (Fig. 26).

Loss of Per-^3H–Labeled Material from Transforming CBs

CBs lost 43 ± 13 and 63 ± 4% of the Per-NaB^3H_4–labeled material when they transformed for 1 and 3 h, respectively. LMARG of radiolabeled CBs showed that 45% of the surface radioactivity was lost when organisms transform for 1 h (Table

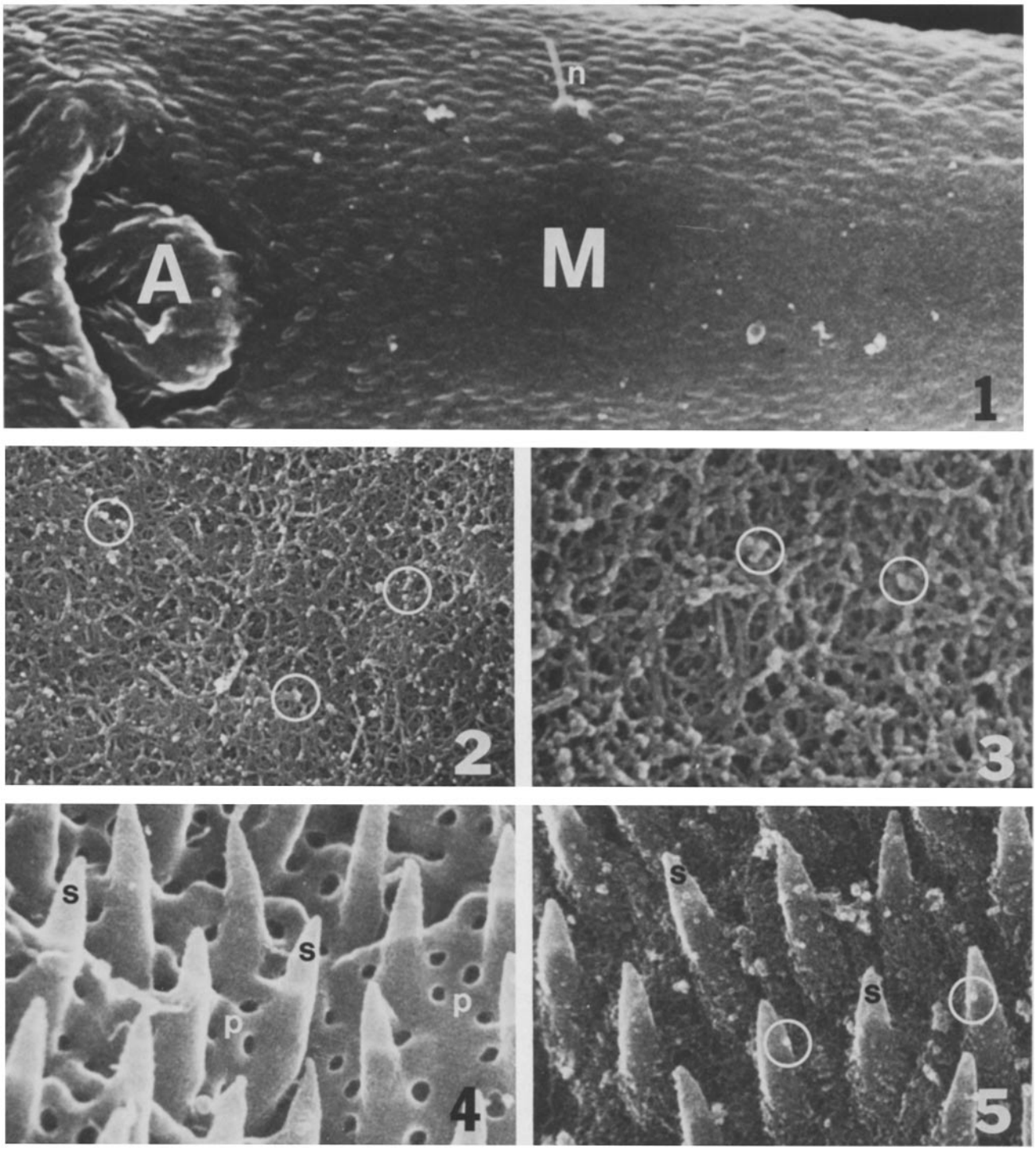

FIGURES 1–5 Scanning micrographs of cercariae and CBs. Glycocalyx covers the surface of a CB so that spines are barely seen on the acetabulum (*A*) and on the middle body (*M*, Fig. 1). A ciliated nerve ending (*n*) projects through the glycocalyx. Over the middle (Fig. 2) and posterior (Fig. 3) CB, the glycocalyx is a fibrillar mesh, composed of 15–30-nm fibrils and spheres (circles). The glycocalyx is absent on a cercaria fixed without osmium (Fig. 4) so that naked spines (*s*) and pits (*p*) 0.2 μm in diameter are seen. After aggregation in their secretions (Fig. 5), parasites also lose glycocalyx so that spines are visible. (Fig. 1) × 5,000. (Figs. 2, 4, and 5) × 25,000. (Fig. 3) × 50,000.

I). There was no increase in radioactivity on the interior of parasites, which suggests that surface material was shed. On SDS PAGE, 77 ± 16% of the radioactivity in the pellet of organisms was retained in the stack, whereas the remaining material ran with the front. Similarly, 97 ± 3% of the radioactivity released into the medium by cultured CBs was retained in the stack of SDS PAGE. On Sepharose 2B, 66 ± 6% of radioactivity eluting at V_0-R_f 0.5 remained with pelleted CBs transforming for 1 h, whereas 34% was found in the medium. After 3 h, 33 ± 6% of the radioactivity at V_0-R_f 0.5 remained with the pellet and 67% was recovered in the medium (Fig. 27). At the same time, radioactivity eluting at V_t accounted for only 16 ± 10% of the total radioactivity (Fig. 27), which suggests that there had been no degradation of

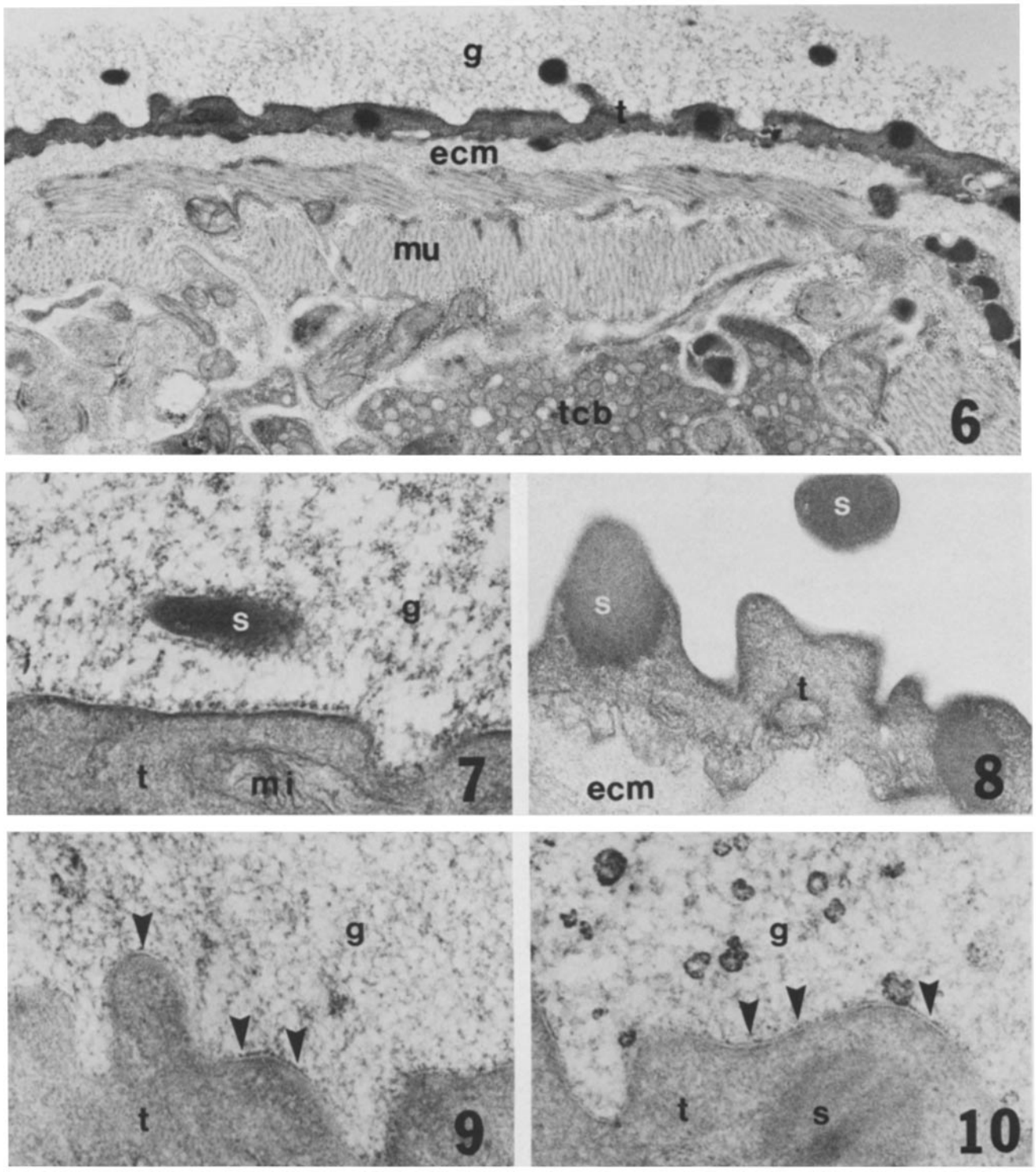

FIGURES 6–10 Transmission micrographs of the surface of cercariae. The cercarial tegument (*t*) is a 0.2–1.0-μm thick syncytium that overlies extracellular matrix (*ecm*), muscle (*mu*), and tegumental cell bodies (*tcb*) filled with membranous vesicles (Fig. 6). The tegument itself contains spines (*s*) and mitochondria (*mi*, Fig. 7). The glycocalyx (*g*) appears as a 1–2-μm-thick fibrillar mesh when it is stained with IRS (Figs. 6 and 7), tannic acid (Fig. 9), or ruthenium red (Fig. 10). The glycocalyx is poorly visualized when fixed initially with mixed aldehydes alone (Fig. 8). The surface of cercariae and nontransforming CBs is bound by a single unit membrane (arrowheads, Figs. 9 and 10). (Fig. 6) × 21,000. (Figs. 7 and 8) × 58,000. (Figs. 9 and 10) × 100,000.

high molecular weight material. In contrast, 91 ± 5% of the Per-NaB^{3}H$_4$–labeled material was retained by CBs incubated in RPMI plus ES, which inhibited transformation. Less than 8% of the radioactivity eluting at V_0-R_f 0.5 was released into the medium, and radioactivity at V_t was ~13% of the total radioactivity.

Labeling with Iodogen-Na^{125}I

Cercariae treated with Iodogen-Na^{125}I bound 50 times the radioactivity of organisms treated with Na^{125}I alone. On LMARG, both surface and internal grain density on Iodogen-Na^{125}I organisms were greatly increased as compared with

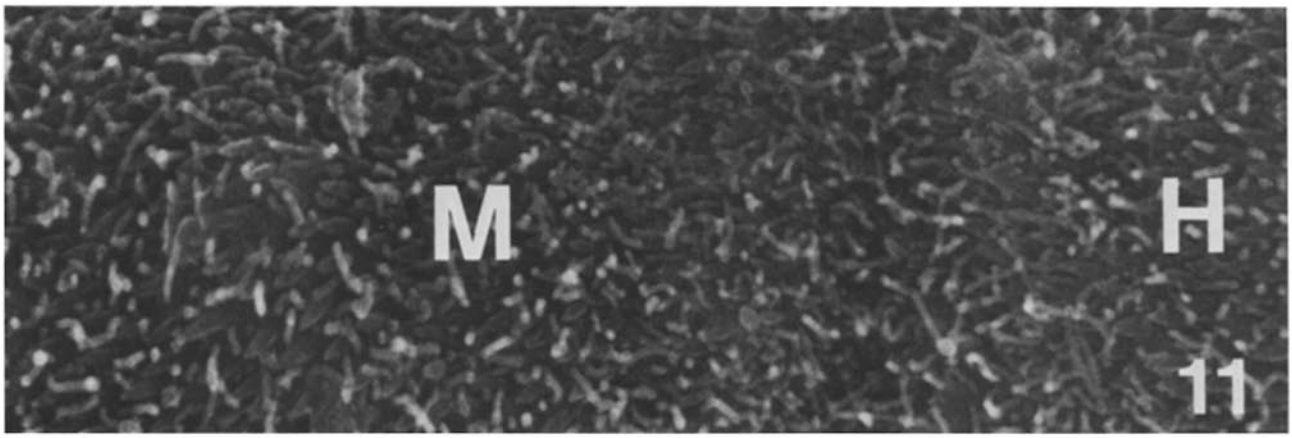
M
H
11

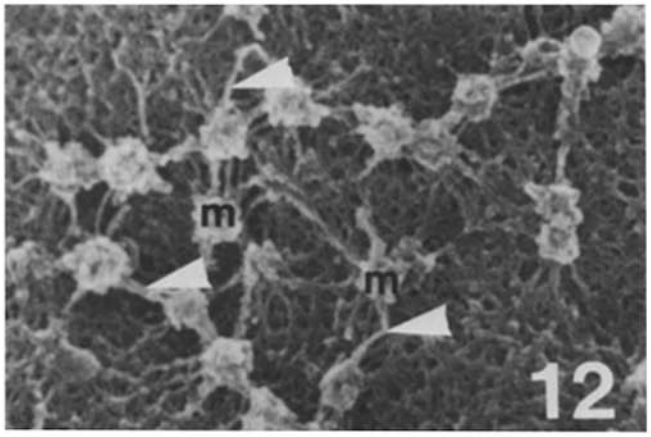
m
m
12

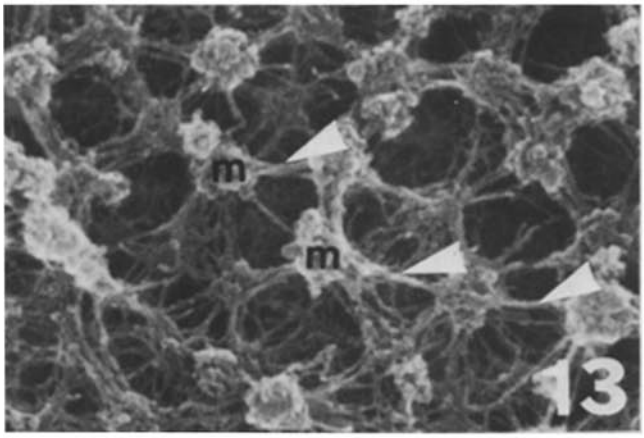
m
m
13

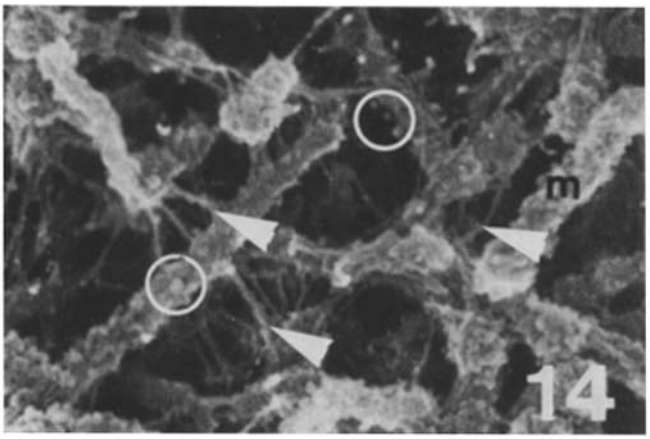
m
14

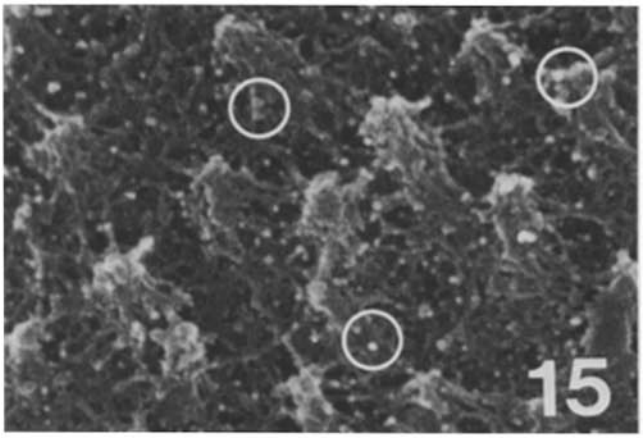
15

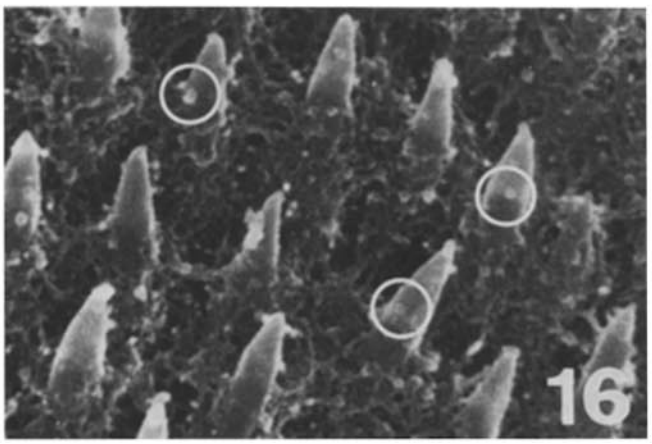
16

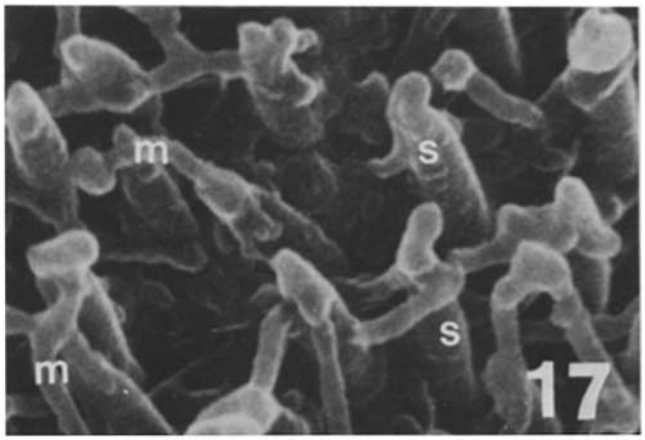
m
s
s
m
17

controls with $Na^{125}I$ alone. More than 80% of the incorporated radioactivity was extractable with chloroform and methanol (2:1) and was presumably bound to lipid. Most of the remaining Iodogen-$Na^{125}I$-labeled material was retained in the stack of reduced SDS PAGE (Fig. 23). No radioactivity was found in the stack when organisms were treated with $Na^{125}I$ only. The high molecular weight material was specifically precipitated by IRS (Fig. 24), and 78 ± 3% of this material was released into the medium by CB transformed for 1 h.

Light Microscopic Studies

Cercariae oxidized with periodate and then treated with FITSC bound $10 \pm 3 \times 10^9$ molecules fluorescein/organism, or $\sim 5 \times 10^5$ molecules/μm^2 surface area. Unoxidized parasites bound only 4% of the FITSC bound to Per-treated organisms. On the Sepharose column, 10–25% of the FITSC eluted with V_0 and the rest with V_t. This may indicate instability of the linkage between the sugar and fluorochrome over time as is seen in other systems (40). Fluorescein was seen diffusely over the surface of the body and tail of cercariae, and the spines appeared black against the bright background (Fig. 28). The amount of fluorescein on the body varied and was greatest posteriorly (Fig. 28). The anterior body emitted 46 ± 12% the fluorescence of the posterior body, the middle body 75 ± 12%, and the tail 55 ± 16%.

CBs lost 46 ± 8% of the FITSC when they transformed for 1 h. On 85 ± 10% of the parasites, a fluorescent corona extended 3–4 μm from the surface (Fig. 29). Within the corona, microvilli projected perpendicularly from the parasite surface (Fig. 30). Motile, transforming CBs deposited fluorescent patches, that contain material visible by interference-contrast microscopy (Figs. 31 and 32).

Rhodamine-conjugated IRS-labeled CBs also formed a fluorescent corona on their surface during transformation (Fig. 33). FICon A did not bind to the cercarial glycocalyx but only to the anterior tip of the parasite, where gland ducts open to the exterior. When CBs transformed for 1 h, FICon A bound in a reticular fashion to CBs, with more fluorescence at the head than at the posterior body (Fig. 34). After 3 h, FICon A bound to the entire surface of the schistosomula (4).

DISCUSSION

The cercarial glycocalyx is a 1–2-μm thick mesh of 15–30 nm fibrils that envelops the organism. Radiolabeled and detergent solubilized glycocalyx has a molecular weight in the millions and an isoelectric point of 5, and is antigenic. The meshwork is partially removed by cercarial secretions and by shedding of the cercarial membrane via microvilli during transformation to schistosomula. However, several hours after transformation, fibrillar material 0.1–0.5-μm thick overlies the double membrane surface of schistosomula and organisms retain >30% of the radiolabeled glycocalyx.

Intact Cercarial Glycocalyx

The glycocalyx is a labile structure, which is difficult to demonstrate by scanning microscopy. Previous studies have failed to visualize it because of the omission of osmium postfixation (7, 42, 58), or perhaps because of the extensive loss of glycocalyx that occurs when cercariae secrete and aggregate (33). The lability of the coat extends also to transmission microscopy, where we failed to visualize the glycocalyx with conventional fixatives. However, others, using higher aldehyde concentrations, have seen a fibrillar coat similar to that shown in Figs. 6–10 (20, 24, 48). In addition, the glycocalyx is consistently demonstrated when stained by ruthenium red, tannic acid, or antibody (25, 26), and by techniques that depend upon periodate oxidation (24, 52, 53). These staining properties suggest that the glycocalyx may be a complex carbohydrate such as a proteoglycan or a lipopolysaccharide. The glycocalyx covers the spines, as shown by transmission microscopy, but the fibrils are 8–15 nm rather than 15–30 nm as seen by scanning. This difference is probably due to the coat of gold-palladium on scanning samples.

The high molecular weight material labeled by Per-NaB^3H_4 is most likely the cercarial glycocalyx. First, LMARG localized radioactivity to the parasite surface. Second, Per-FITSC fluorescence was greater on the posterior body than the anterior body or tail, which is the same distribution as the fibrillar mesh seen by scanning microscopy. Third, IRS, which binds specifically to the glycocalyx, precipitated Per-NaB^3H_4 labeled material. Fourth, the mesh, the radiolabel, and FITSC were all lost during transformation. Finally, Iodogen-$Na^{125}I$ labeled similar high molecular weight material on cercariae, which suggests that this is the major moiety on the parasite surface. The radiolabeled glycocalyx had a molecular weight of $>10^6$ and an isoelectric point of 5. Because the glycocalyx is labeled by Per-NaB^3H_4 and by iodination, it may contain sialic acid (15) and tyrosine, histidine, or lipid (21, 31).

Loss of the Glycocalyx with Transformation

During transformation, the cercarial membrane is lost through the formation and shedding of microvilli, as has been previously suggested (20, 33). Microvilli synchronously arose and elongated when tails are lost and CBs were placed in saline. By the time microvilli were shed at 40–60 min, they reached an average length of ~4 μm. Since the villous diameter was ~0.15 μm and there were 2 villi per μm^2 surface areas, ~4 μm^2 membrane/μm^2 surface was shed. This suggests that some new membrane as well as the original cercarial membrane was incorporated into the microvilli. The single membrane removed by the loss of the microvilli is replaced by a double membrane system transported to the tegument in multilamellar bodies from the syncytial cell bodies beneath the muscle (20, 61). In the first hour after transformation, both single and double membranes are present on the tegument surface (20).

FIGURES 11–17 Scanning micrographs of CB transforming to schistosomula. Within 10 min in RPMI, CBs form microvilli over their head (*H*) and middle body (*M*, Fig. 11). Microvilli (*m*) are short at 5 min (Fig. 12), and elongate to 2–3-μm at 10 min (Fig. 13) and 3–5 μm at 20 min (Fig. 14). Microvilli are at first an apex for the attachment glycocalyx fibrils (arrowheads, Figs. 12 and 13) but appear later to separate the glycocalyx (arrowheads, Fig. 14). Long microvilli are covered by 15–30-nm spheres (circles, Fig. 14). Microvilli are absent after 40–60 min (Fig. 15), although much glycocalyx remains and obscures spines. 3 h after transformation, schistosomula still have fibrillar material in areas between spines (Fig. 16). Without osmification, the spines (*s*) and microvilli are naked (Fig. 17). (Fig. 11) × 6,500. Figs. 12–17 are all of the posterior body; × 25,000.

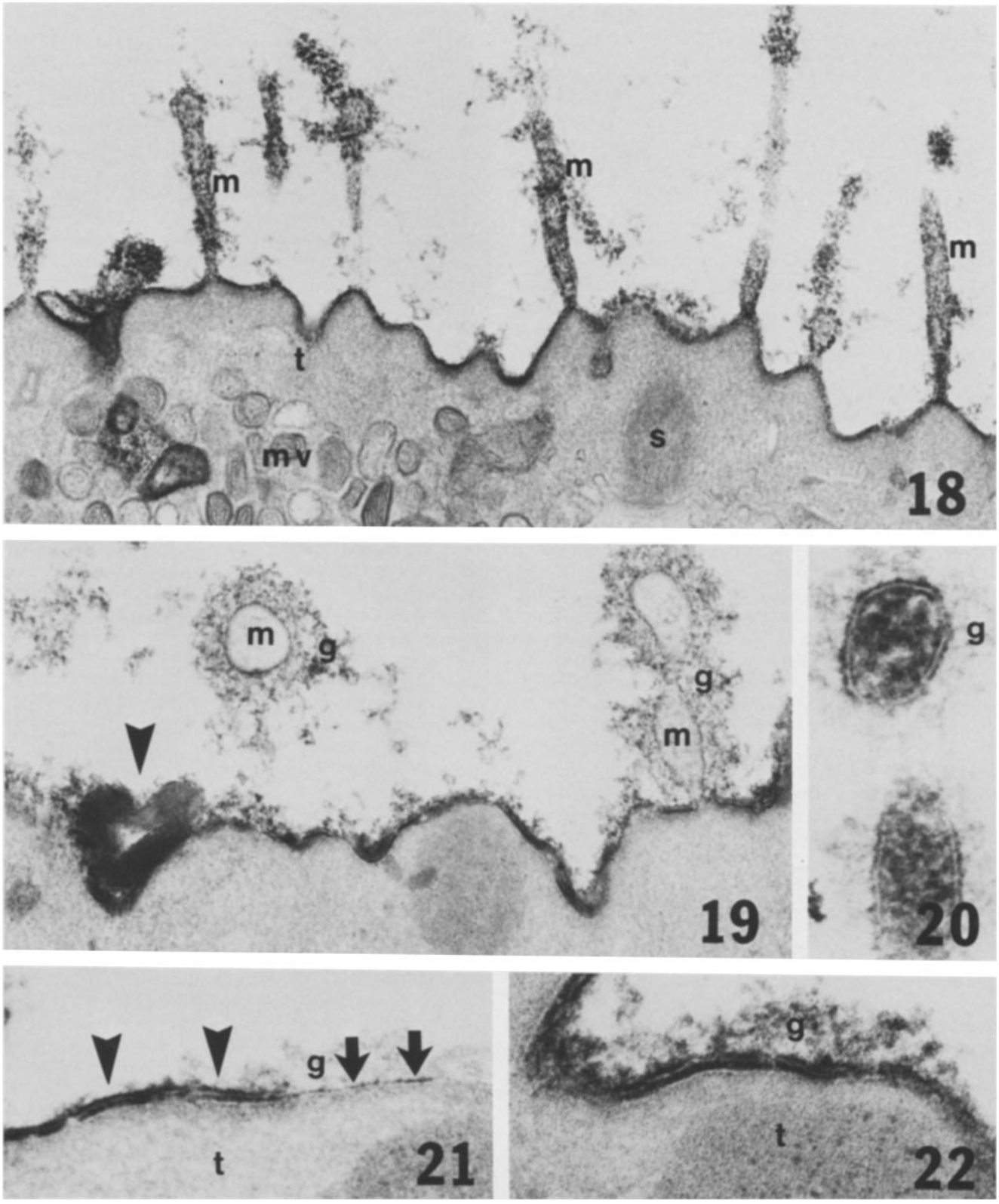

FIGURES 18–22 Transmission micrographs of transforming CBs. The surface of a CB transforming for 30 min is covered with microvilli (*m*, Fig. 18). Within the tegument (*t*) are spines (*s*) and multilaminate vesicles (*mv*), which discharge onto the tegumental surface (arrowhead, Fig. 19). Microvilli are 0.1 μm in diameter, covered with a dense coat of glycocalyx (*g*), and bound by a single unit membrane (Fig. 20). After 30 min, areas of single unit membrane (arrows, Fig. 21) alternate with areas of double unit membrane (arrowheads, Fig. 21) on the tegumental surface. After 60 min, fibrillar glycocalyx is still present on the double unit membrane, which covers the parasite surface (Fig. 22). CBs in Figs. 18, 19, and 22 are stained with antibody, in Figs. 20 and 21 with tannic acid. (Fig. 18) × 50,000. (Fig. 19) × 80,000. (Fig. 20) × 103,000. (Fig. 21) × 140,000. (Fig. 22) × 180,000.

TABLE I

Light Microscopic Autoradiography of Per-labeled Cercariae

Preparation	Grain density: Interior (I)	Surface (S)	S/I	Absolute No. S/I
CB NaB^3H_4 only	1.8 ± 0.4	1.3 ± 0.5	0.7 ± 0.2	0.27 ± 0.1
CB Per-NaB^3H_4 Intact	1.7 ± 0.4	16.1 ± 5.7	9.6 ± 2.6	3.4 ± 1.0
	$P = 0.5$	$P < 0.001$	$P < 0.001$	$P < 0.001$
Transformed Cercariae Per-NaB^3H_4	1.3 ± 0.3	8.9 ± 2.9	6.5 ± 2.0	1.3 ± 0.3
	1.3 ± 0.3	22.7 ± 7.2	34.0 ± 13	12.3 ± 2.8
	$P = 0.06$	$P < 0.001$	$P < 0.001$	$P < 0.001$

Grain density = No. of grains per 100 μm^2. Values represent the mean ± SD of 30–50 organisms for each condition. *P* values show the significance (Student's *t*-test) of differences between values of Per-NaB^3H_4-labeled organisms and organisms treated with NaB^3H_4 alone. CBs were transformed for 1 h. For LMARG, CBs were labeled in the cold and so may have lost some of their glycocalyx when they aggregated in their own secretions. The density of radioactivity on the surface of CBs (16.1) is, therefore, somewhat less than that on cercariae labeled in the presence of ES (22.7).

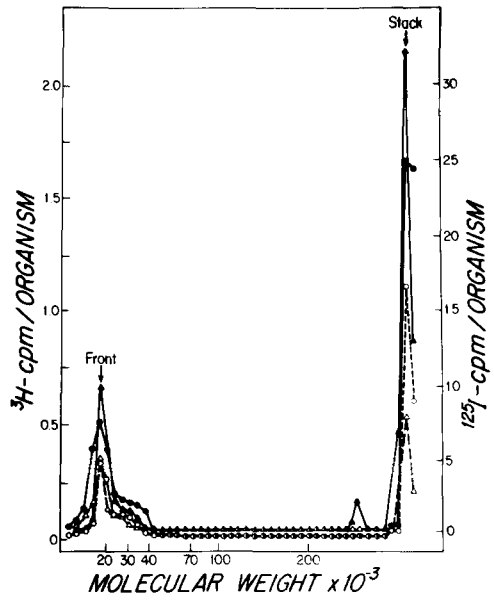

FIGURE 23 Representative SDS PAGE of cercariae and CBs labeled with Per-NaB^3H_4 and Iodogen-$Na^{125}I$. Per-NaB^3H_4-labeled material from cercariae (●) and CBs (○) remains predominantly in the stack of tube gels containing 5% acrylamide and Laemmli buffer, with ~20% of the radioactivity running with the dye front. Chloroform-methanol extracts of Iodogen-$Na^{125}I$-labeled cercariae (▲) or CBs (△) also show radioactivity remaining in the stack. Similar results occurred with phosphate-buffered SDS PAGE. Control parasites incubated with NaB^3H_4 or $Na^{125}I$ alone have no radioactivity in the stack (not shown).

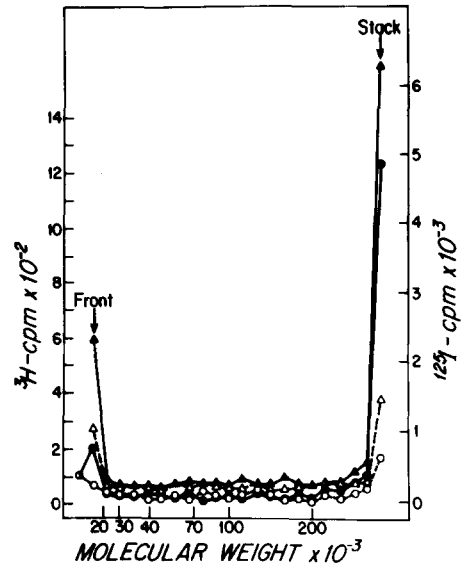

FIGURE 24 IRS precipitates of Per-Na^3H_4 (●) and Iodogen-$Na^{125}I$ (▲) labeled material also remain in the stack of SDS PAGE. In contrast, precipitations with NRS show little NaB^3H_4 (○) and $Na^{125}I$ (△) in the stack.

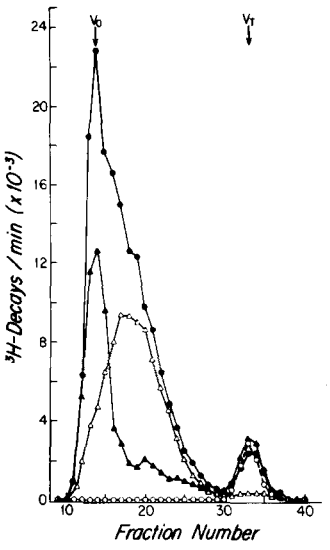

FIGURE 25 Representative Sepharose 2B chromatograms of Per-NaB^3H_4-labeled cercariae. Some 70–90% of the radioactivity from cercariae (●) elutes as a peak at the void volume (V_0) with a broad shoulder extending to R_f 0.5, and 10–30% radioactivity elutes with the total volume (V_t). Per-NaB^3H_4 from CBs (▲) elutes with V_0, whereas Per-NaB^3H_4 from tails (△) elutes with an R_f of 0.2–0.3. Control organisms (○) incubated with NaB^3H_4 alone have radioactivity that elutes entirely with V_t. On the same column, dextran averaging 2 × 10^6 mol wt and immunoglobulin of 1.5 × 10^5 mol wt have peaks at R_f 0.5 and 0.85, respectively.

The loss of the glycocalyx is a complex process that appears to involve at least three mechanisms. First, the mesh on the surface of cercariae becomes thinner when parasites in APW aggregate in secreted mucus. This loss is independent of membrane changes, because these cercariae retain a single unit membrane. The loss is apparently caused by glandular secretions, because the loss, secretion, and aggregation are all inhibited by ES. Second, 30–50% of the glycocalyx is lost during the time that microvilli are formed and shed (20). Third, after microvilli have been shed at 1 h, there is a continued loss of the glycocalyx. This loss may be due not only to glandular secretion, but also to surface membrane turnover, which is occurring with a halftime of 10–12 h (43). The lost glycocalyx can be recovered from the medium and is still of high molecular weight, suggesting that it is sloughed largely intact (43, 45). This conclusion is supported by both LMARG, where no radioactivity is internalized by transforming organisms, and by the observation of fluorescent glycocalyx shed onto the slide.

Residual glycocalyx was present on schistosomula chemically and ultrastructurally, which agrees with previous studies of schistosomula transforming in rodent skin (20, 53). However, the glycocalyx on both skin and mechanically transformed parasites appeared thicker than was previously demonstrated (2, 6, 7). The glycocalyx retained on schistosomula, which is of high molecular weight, and excluded from SDS PAGE, appears to have been labeled on schistosomula by iodination (49) or by NaB^3H_4 after oxidation with periodate or galactose oxidase (43). It is unlikely that the glycocalyx or its cleavage products account for the dozen or so proteins

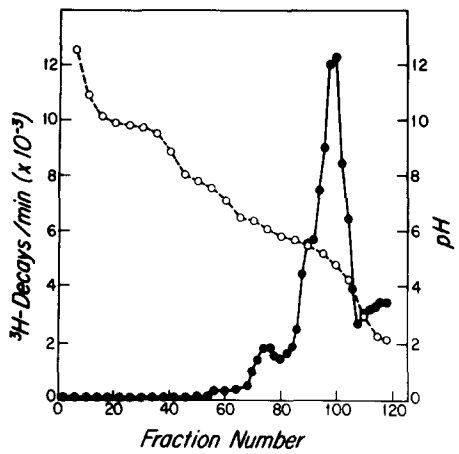

FIGURE 26 Representative isoelectric focusing of Per-NaB^{3}H$_4$-labeled cercariae. Radioactivity (●) and pH (○) are plotted vs. fraction number. 10,000 labeled organisms were solubilized in NP40 and urea, loaded onto the sucrose column at pH 7, and electrophoresed for 80,000 V·h. The anode was at the top of the column. Samples solubilized in SDS and β-mercaptoethanol and samples focused on a flatbed gel also moved toward the anode.

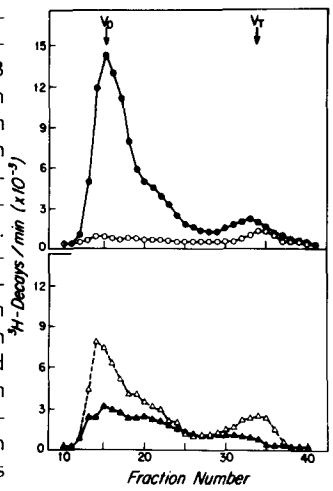

FIGURE 27 Representative Sepharose 2B chromatograms of transforming CBs. CB incubated for 3 h in the presence of ES, which inhibits transformation, retain Per-NaB^{3}H$_4$-labeled material on their surface (●) and do not release high molecular weight material into the medium (○) (*top*). Less than 10% of the total radioactivity associated with CBs cultured with ES is seen at V_t. In contrast, 3 h after transformation 67% of the Per-NaB^{3}H$_4$-labeled material is found in the medium (△) and elutes at V_0–R_f 0.5 (*bottom*). Radioactivity retained on transformed CBs after 3 h (▲) is predominantly of high molecular weight. Radioactivity at V_t remains at <10% of the entire radioactivity, which indicates that there is little degradation.

ranging from 17,000 to 110,000 mol wt previously identified on schistosomula (12, 43, 49, 57). These proteins are probably specific for the schistosomular membranes. The binding of concanavalin A to schistosomula but not to cercariae also suggests that there are surface components expressed only after transformation.

Immunological Relevance

The surface of cercariae is antigenic (24–26, 51, 55, 59) and activates complement by the alternative pathway (8, 11, 39). The high molecular weight acidic material labeled here appears to be the major cercarial surface antigen. It is possible that residual cercarial glycocalyx accounts for a sizable fraction of the antibody and/or complement binding sites on the surface of schistosomula, as well as of cercariae (9, 10, 32, 39, 46). The loss of residual glycocalyx may coincide with a decrease in antibody binding and complement fixation and may account for the increasing resistance of developing schistosomula to immune attack (9, 10, 39, 46). Consistent with this hypothesis, mice injected with irradiated cercariae are better protected against reinfection than are those exposed to irradiated schistosomula (47). However, other smaller antigens have been identified on the surface of schistosomula (12, 13, 18, 57) and recently monoclonal antibodies to two of these antigens have been shown to be protective in rats (13) and mice (18).

The corona of FITSC and rhodamine-conjugated IRS on transforming CBs resembles the cercarienhüllen reaktion, a light microscopic assay for schistosomiasis (51, 55, 59). Living cercariae incubated in saline with patient sera with or without complement for 1–5 h form a 3–4-μm-thick surface coat in immune but not in normal sera. We speculate that cercariae transform in saline in a poorly synchronized fashion and that visualization of the cercarienhüllen reaktion depends upon the binding of enough antibody and complement to render the shedding glycocalyx refractile. In the same way, antibody and complement appear to stabilize the glycocalyx for scanning microscopy in the absence of osmium (58).

The authors thank Dr. Donald Harn for his gift of the IRS and Drs. David Golan and Will Veatch for suggesting the use of the fluoresceinthiosemicarbazide technique. We are grateful to Ms. Dee Condon for excellent secretarial assistance and thank also Mrs. Ann Hein and Dr. Shona McDiarmid for helpful comments on the manuscript.

Dr. Samuelson was supported by National Institutes of Health (NIH) Medical Scientist Training Program grant GM 07753. Dr. Caulfield is the recipient of an NIH Career Development Award, AM 00775. This work was supported by NIH grant AI 19581 and a grant from the Edna McConnell Clark Foundation.

Received for publication 5 June 1984, and in revised form 7 January 1985.

REFERENCES

1. Barker, L. R., E. Bueding, and A. R. Timms. 1966. The possible role of acetylcholine in *Schistosoma mansoni*. *Br. J. Pharmacol.* 26:656–665.
2. Brink, L. H., D. J. McLaren, and S. R. Smithers. 1977. *Schistosoma mansoni*: a comparative study of artificially transformed schistosomula and schistosomula recovered after cercarial penetration of isolated skin. *Parasitology.* 74:73–86.

FIGURES 28–34 Light micrographs of cercariae and transforming CBs. The surface of a Per-FITSC-labeled cercaria (Fig. 28) is diffusely fluorescent with the posterior body appearing brightest. Areas of the head (*H*), middle (*M*), posterior (*P*) body, and tail (*T*) measured with the photometer are marked. Spines are seen as black dots and are more dense on the body than on the tail. Cercariae incubated with FITSC alone do not fluoresce (not shown). A CB transforming for 30 min (Fig. 29) has a fluorescent corona (arrowheads), which is thickest on the posterior body (*P*). Interference-contrast microscopy of the same organism (Fig. 30) shows that microvilli project perpendicular to the parasite surface in regions of the corona (arrowheads). Transforming CBs are motile and shed fluorescent material (Fig. 31), which is fibrillar (arrow) and globular (arrowheads). This material is also visible by interference-contrast microscopy (Fig. 32). A CB incubated with rhodamine-conjugated IRS and transformed for 30 min also has a fluorescent corona (arrowheads, Fig. 33) on its posterior body (*P*). A CB transformed for 1 h binds FlCon A in a reticular fashion over its posterior body (Fig. 34). Spines appear as bright dots. (Fig. 28) × 700. (Figs. 29–34) × 875.

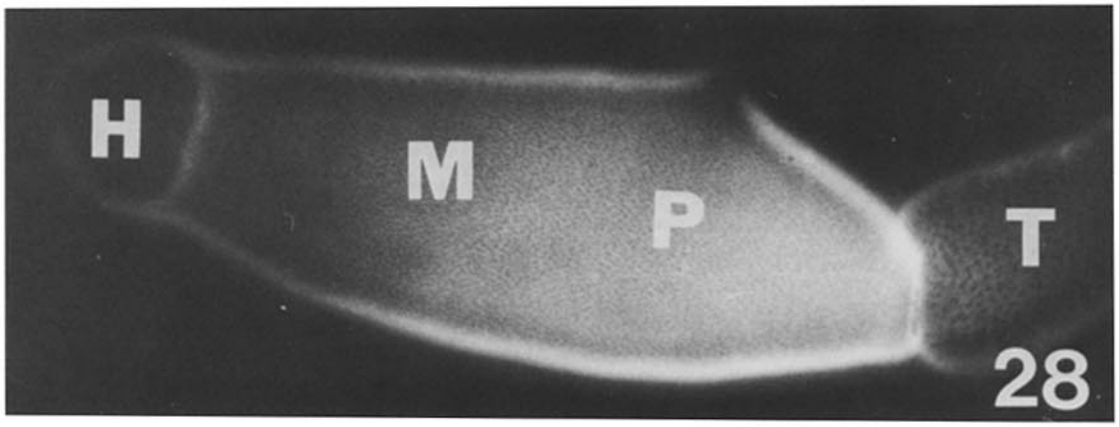
H
M
P
T
28

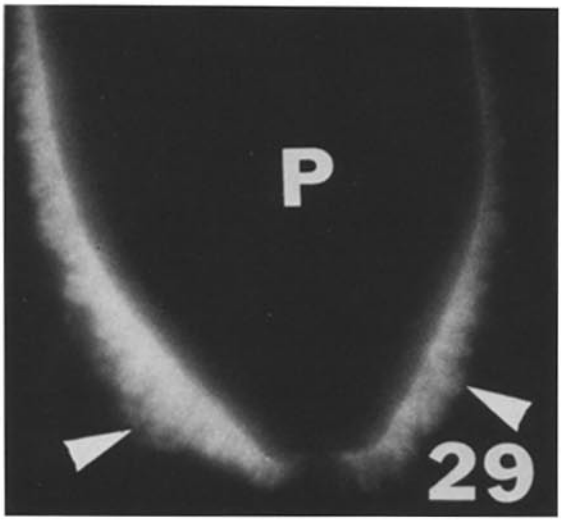
P
29

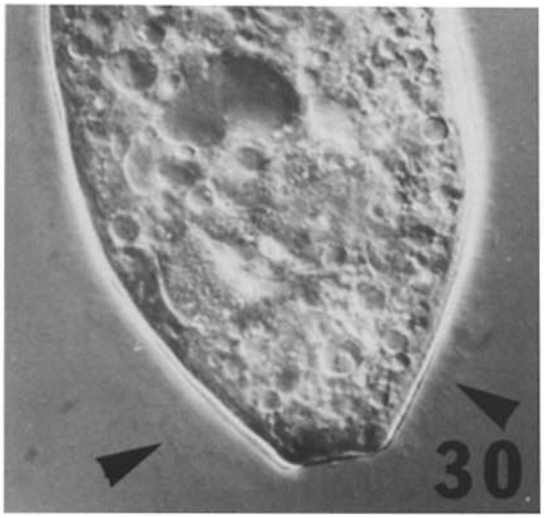
30

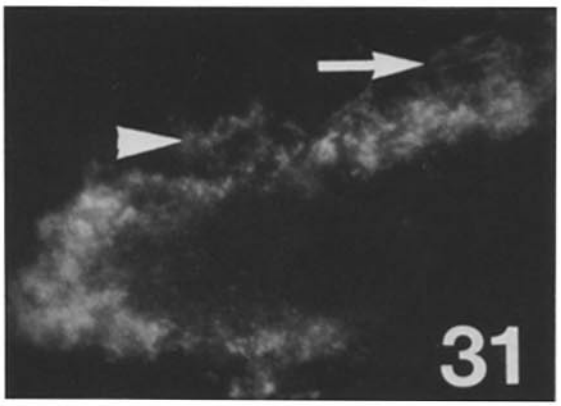
31

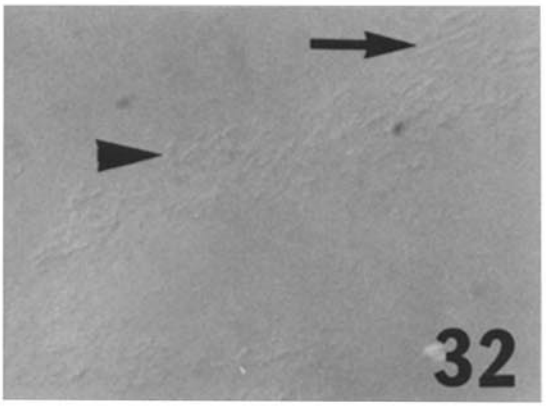
32

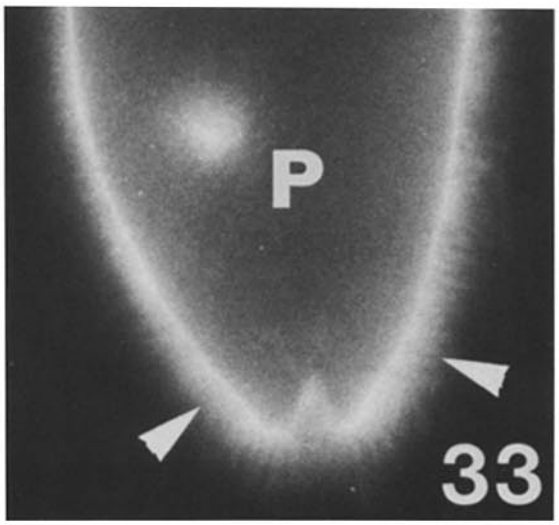
P
33

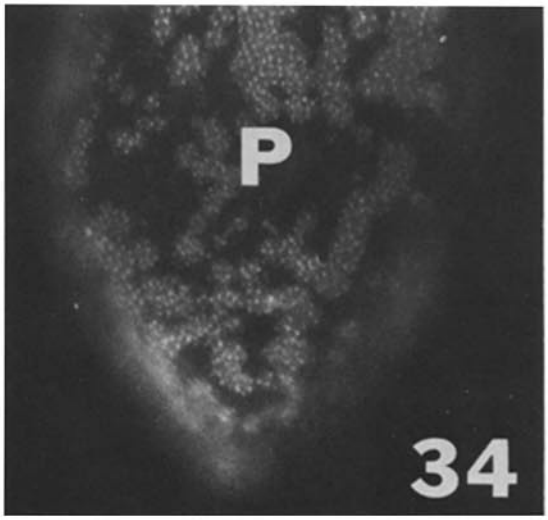
P
34

3. Butterworth, A. E. 1977. The eosinophil and its role in immunity to helminth infections. *Curr. Top. Microbiol. Immunol.* 77:127–168.
4. Caulfield, J. P., G. Korman, and J. C. Samuelson. 1982. Human neutrophils endocytose multivalent ligands from the surface of schistosomula of *S. mansoni* before membrane fusion. *J. Cell Biol.* 94:370–378.
5. Colley, D. G., and S. K. Wikel. *Schistosoma mansoni*: simplified method for the production of schistosomules. *Exp. Parasitol.* 35:44–51.
6. Cousin, C. E., M. A. Stirewalt, and C. H. Dorsey. 1982. *Schistosoma mansoni*: ultrastructure of early transformation of skin- and shear-pressure-derived schistosomules. *Exp. Parasitol.* 51:341–365.
7. Crabtree, J. E., and R. A. Wilson. 1980. *Schistosoma mansoni*: a scanning electron microscope study of the developing schistosomulum. *Parasitology.* 81:553–564.
8. Culbertson, J. T. 1936. The cercaricidal action of normal serums. *J. Parasitol.* 22:111–125.
9. Dean, D. A. 1977. Decreased binding of cytotoxic antibody by developing *Schistosoma mansoni*. Evidence for a surface change independent of host antigen absorbtion and membrane turnover. *J. Parasitol.* 63:418–426.
10. Dessein, A., J. C. Samuelson, A. E. Butterworth, M. Hogan, B. A. Sherry, M. A. Vadas, and J. R. David. 1981. Immune evasion by *Schistosoma mansoni*: loss of susceptibility to antibody or complement-dependent eosinophil attack by schistosomula cultured in medium free of macromolecules. *Parasitology.* 82:357–374.
11. Dias da Silva, W., and M. D. Kazatchkine. 1980. *Schistosoma mansoni*: activation of the alternative pathway of human complement by schistosomula. *Exp. Parasitol.* 50:278–286.
12. Dissous, C., C. Dissous, and A. Capron. 1981. Isolation and characterization of surface antigens from *Schistosoma mansoni* schistosomula. *Mol. Biochem. Parasitol.* 3:215–225.
13. Dissous, C., J.-M. Grzych, and A. Capron. 1982. *Schistosoma mansoni* surface antigen defined by a rat monoclonal IgG2a. *J. Immunol.* 129:2232–2234.
14. Fischer, L. 1969. An introduction to gel chromatography. *In* Laboratory Techniques in Biochemistry and Molecular Biology. Vol. 1. T. S. Work and E. Work, editors. North Holland Publishing Co., Amsterdam.
15. Gahmburg, C. G., and L. C. Andersson. 1977. Selective radioactive labeling of cell surface sialoglycoproteins by periodate-tritiated borohydride. *J. Biol. Chem.* 252:5888–5894.
16. Golan, D. E., P. Singer, and W. R. Veatch. 1984. Calcium-induced immobilization of glycophorin in the human erythrocyte membrane. *Biophys. J.* 45:202a. (Abstr.)
17. Gordon, R. M., and R. B. Griffiths. 1951. Observations on the means by which the cercariae of *Schistosoma mansoni* penetrate mammalian skin, together with an account of certain morphological changes observed in the newly penetrated larvae. *Ann. Trop. Med. Parasitol.* 45:227–243.
18. Harn, D. A., M. Mitsuyama, and J. R. David. 1984. *Schistosoma mansoni*: anti-egg monoclonal antibodies protect against cercarial challenge in vivo. *J. Exp. Med.* 159:1371–1387.
19. Hasty, D. L., and E. D. Hay. 1978. Freeze-fracture studies of the developing cell surface. II. Particle-free membrane blisters on glutaraldehyde-fixed corneal fibroblasts are artefacts. *J. Cell Biol.* 78:756–768.
20. Hockley, D. J., and D. J. McLaren. 1973. *Schistosoma mansoni*: changes in the outer membrane of the tegument during development from cercaria to adult worm. *Int. J. Parasitol.* 3:13–25.
21. Hubbard, A. L., and Z. A. Cohn. 1975. Externally disposed plasma membrane proteins. I. Enzymatic iodination of mouse L cells. *J. Cell Biol.* 64:438–460.
22. Karnovsky, M. J. 1965. A formaldehyde-glutaraldehyde fixative of high osmolarity for use in electron microscopy. *J. Cell Biol.* 27:137a.
23. Kassim, O., and D. E. Gilbertson. 1976. Hatching of *Schistosoma mansoni* eggs and observations on motility of miracidia. *J. Parasitol.* 62:715–720.
24. Kemp, W. M. 1970. Ultrastructure of the cercarienhullen reaktion of *Schistosoma mansoni J. Parasitol.* 56:713–723.
25. Kemp, W. M. 1972. Serology of the Cecarienhüllen Reaktion of *Schistosoma mansoni. J. Parasitol.* 58:686–692.
26. Kemp, W. M., R. T. Damian, and N. D. Greene. 1973. *Schistosoma mansoni*: immunohistochemical localization of the CHR reaction in the glycocalyx of cercaria. *Exp. Parasitol.* 33:27–33.
27. Kessler, S. W. 1975. Rapid isolation of antigens from cells from a staphylococcal protein A-antibody adsorbent: parameters of the interaction of antibody-antigen complexes with protein A. *J. Immunol.* 115:1617–1624.
28. Laemmli, U. K. 1970. Cleavage of structural proteins during the assembly of the head of bacteriophage T4. *Nature (Lond.).* 227:680–685.
29. Lazdins, J. K., M. J. Stein, J. R. David, and A. Sher. 1982. *Schistosoma mansoni*: rapid isolation and purification of schistosomula of different developmental stages by centrifugation on discontinous density gradients of Percoll. *Exp. Parasitol.* 53:105–116.
30. Luft, J. H. 1971. Ruthenium red and violet. I. Chemistry, purification, methods of use for electron microscopy and mechanism of action. *Anat. Rec.* 171:347–368.
31. Markwell, M. A. K., and C. F. Fox. 1978. Surface-specific iodination of membrane proteins of viruses and eukaryotic cells using 1,3,4,6-tetrachloro-3α,6α-diphenylglycoluril. *Biochemistry.* 17:4807–4817.
32. McLaren, D. J., J. A. Clegg, and S. R. Smithers. 1975. Acquisition of host antigens by young *Schistosoma mansoni* in mice: correlation with failure to bind antibody *in vitro*. *Parasitology.* 70:67–75.
33. McLaren, D. J., and D. J. Hockley. 1976. *Schistosoma mansoni*: the occurrence of microvilli on the surface of the tegument during transformation from cercaria to schistosomulum. *Parasitology.* 73:169–187.
34. Maupin, P., and T. D. Pollard. 1983. Improved preservation and staining of HeLa cell actin filaments, clathrin-coated membranes, and other cytoplasmic structures by tannic acid-glutaraldehyde-saponin fixation. *J. Cell Biol.* 96:51–62.
35. O'Farrelll, P. H. 1975. High resolution two-dimensional electrophoresis of protein. *J. Biol. Chem.* 250:4007–4021.
36. Phillips, S. M., and D. G. Colley. 1978. Immunologic aspects of host responses to schistosomiasis: resistance, immunopathology and eosinophil involvement. *Prog. Allergy* 24:49–182.
37. Radola, B. J. 1973. Isoelectric focusing in layers of granulated gels. I. Thin-layer isoelectric focusing of proteins. *Biochim. Biophys. Acta.* 295:412–428.
38. Ramalho-Pinto, F. J., G. Gazzinelli, R. E. Howells, T. A. Mota-Santos, E. A. Figueiredo, and J. Pelligrino. 1974. *Schistosoma mansoni*: defined system for a stepwise transformation of cercaria to schistosomule *in vitro*. *Exp. Parasitol.* 36:360–372.
39. Ramalho-Pinto, F. J., D. J. McLaren, and S. R. Smithers. 1978. Complement-mediated killing of schistosomula of *Schistosoma mansoni* by rat eosinophils in vitro. *J. Exp. Med.* 147:147–156.
40. Rando, R. R., and F. W. Bangerter. 1979. On the labeling of oxidized cell surface membrane by acyl hydrazides. *Biochem. Biophys. Acta.* 557:354–362.
41. Reynolds, E. S. 1963. The use of lead citrate at high pH as an electron opaque stain in electron microscopy. *J. Cell Biol.* 17:208–212.
42. Robson, R. T., and D. A. Erasmus. 1970. The ultrastructure, based on stereoscan observations, of the oral sucker of the cercaria of *Schistosoma mansoni* with special reference to penetration. *Z. Parasitenkd.* 35:76–86.
43. Samuelson, J. C., and J. P. Caulfield. 1982. Loss of covalently labeled glycoproteins and glycolipids from the surface of newly transformed schistosomula of *S. mansoni*. *J. Cell Biol.* 94:363–369.
44. Samuelson, J. C., J. P. Caulfield, and J. R. David. 1980. *Schistosoma mansoni*: post-transformational changes in schistosomula grown *in vitro* and in mice. *Exp. Parasitol.* 50:369–383.
45. Samuelson, J. C., J. P. Caulfield, and J. R. David. 1982. Schistosomula of *Schistosoma mansoni* clear concanavalin A from their surface by sloughing. *J. Cell Biol.* 94:355–362.
46. Samuelson, J. C., A. Sher, and J. P. Caulfield. 1980. Newly transformed schistosomula spontaneously lose surface antigens and C3 acceptor sites during culture. *J. Immunol.* 124:2055–2057.
47. Sher, A., and D. Benno. 1982. Decreasing immunogenicity of schistosome larvae. *Parasite Immunol.* 4:101–107.
48. Smith, J. A., E. S. Reynolds, and F. von Lichtenberg. 1969. The integument of *Schistosoma mansoni*. *Am. J. Trop. Med. Hyg.* 18:28–49.
49. Snary, D., M. A. Smith, and J. A. Clegg. 1980. Surface proteins of *Schistosoma mansoni* and their expression during morphogenesis. *Eur. J. Immunol.* 10:573–575.
50. Spurr, A. R. 1969. A low-viscosity epoxy resin embedding medium for electron microscopy. *J. Ultrastruct. Res.* 26:31–43.
51. Standen, O. D. 1952. The in vitro effect of normal and immune serum upon the cercariae of *Schistosoma mansoni*. *J. Helminthol.* 26:25–42.
52. Stein, P. C., and R. D. Lumsden. 1973. *Schistosoma mansoni*: topographical features of cercariae, schistosomula, and adults. *Exp. Parasitol.* 33:499–514.
53. Stirewalt, M. A. 1963. Cercaria vs. schistosomule (*Schistosoma mansoni*): absence of pericercarial envelope in vivo and the early physiological and histological metamorphosis of the parasite. *Exp. Parasitol.* 13:395–406.
54. Stirewalt, M. A. 1974. *Schistosoma mansoni*: cercaria to schistosomule. *Adv. Parasitol.* 12:115–182.
55. Stirewalt, M. A., and A. S. Evans. 1955. Serological reactions in *Schistosoma mansoni* infections. I. Cercaricidal, precipitation, agglutination, and CHR phenomena. *Exp. Parasitol.* 4:123–142.
56. Stirewalt, M. A., D. R. Mannick, and W. A. Fregeau. 1966. Definition and collection of schistosomules of *Schistosoma mansoni*. *Trans. R. Soc. Trop. Med. Hyg.* 60:352–360.
57. Taylor, D. W., E. G. Hayunga, and W. E. Vannier. 1981. Surface antigens of *Schistosoma mansoni*. *Mol. Biochem. Parasitol.* 3:157–168.
58. Van der Linden, P. W. G., H. K. Koerten, and A. M. Deelder. 1982. Scanning electron microscopical observations on antigen-antibody coat formation on mechanically transformed *Schistosoma mansoni* schistosomula. *Z. Parasitenkd.* 68:73–80.
59. Vogel, H., and W. Minning. 1949. Weitere Beobachtungen über die Cercarienhüllen reaktion, eine Serapräzipitation mit lebenden *Bilharzia*-cercarien. *Z. Tropenmed. Parasitol.* 1:378–386.
60. Weber, K., and M. Osborn. 1969. The reliability of molecular weight determinations by dodecyl sulfate-polyacrylamide gel electrophoresis. *J. Biol. Chem.* 244:4406–4412.
61. Wilson, R. A., and P. E. Barnes. 1974. The tegument of *Schistosoma mansoni*: observations on the formation, structure and composition of cytoplasmic inclusions in relation to tegument function. *Parasitology.* 68:239–258.